An energy-efficient plasma methane pyrolysis process for high yields of carbon black and hydrogen

Laurent Fulcheri, Vandad-Julien Rohani, Elliott Wyse, Ned Hardman, Enoch Dames

An Energy-Efficient Plasma Methane Pyrolysis Process for High Yields of Carbon Black and Hydrogen

Laurent Fulcheri[a†], Vandad-Julien Rohani[a] , Elliott Wyse[b], Ned Hardman[b], Enoch Dames[b]

[a]*PSL Research University, MINES ParisTech, PERSEE - Centre Procédés, Énergies renouvelables et Systèmes énergétiques, 1 Rue Claude Daunesse, 06904, Sophia Antipolis, France*

[b]*MONOLITH Materials, 662 Laurel Street, Suite 201 San Carlos, CA 94070*

Submitted to International Journal of Hydrogen Energy

[†]Correspondence concerning this article should be addressed to:

Prof. Laurent FULCHERI

Email: laurent.fulcheri@mines-paristech.fr

Telephone: +33-4-9395-7406

Abstract

A novel thermal plasma process was developed, which enables economically viable commercial-scale hydrogen and carbon black production. Key aspects of this process are detailed in this work. Selectivity and yield of both solid, high-value carbon and gaseous hydrogen are given particular attention. For the first time, technical viability is demonstrated through lab scale reactor data which indicate methane feedstock conversions of >99%, hydrogen selectivity of >95%, solid recovery of >90%, and the ability to produce carbon particles of varying crystallinity having the potential to replace traditional furnace carbon black. The energy intensity of this process was established based on real-time operation data from the first commercial plant utilizing this process. In its current stage, this technology uses around 25 kWh per kg of H2 produced, much less than water electrolysis which requires approximately 60 kWh per kg of H2 produced. This energy intensity is expected to be reduced to 18-20 kWh per kg of hydrogen with improved heat recovery and energy optimization.

Keywords: thermal plasma, carbon black, hydrogen, methane pyrolysis, methane decomposition

1 Introduction

The most common current method of hydrogen production on an industrial scale – Steam Methane Reforming (SMR) – is accompanied by more than 10 tons of CO_{2eq} per ton of hydrogen[1]. Most oil and gas companies are now considering combining SMR with Carbon Capture and Storage (CCS), but this is not yet deployed at industrial scale. Water electrolysis however holds promise as a source of "decarbonized" hydrogen (green H2) when using low-carbon electricity. Unfortunately, water dissociation is extremely energy-intensive since it requires a minimum of 285 kJ per mole, and thus the cost of H_2 from electrolysis remains significantly higher than that produced from SMR.

An additional pathway for H2 production is based on the pyrolysis of methane to produce solid carbon and H_2:

$$CH_4 \rightarrow C + 2\,H_2 \quad 76\ kJ/Mole \qquad (1)$$

The main advantage of this method is that it allows CO_2-free production of hydrogen and solid carbon while being thermodynamically less energy-intensive than water dissociation for H_2 production, requiring about seven times less energy per mass (or mole) of hydrogen (38 kJ vs 285 kJ per mole H2)[2]. Additionally, this process can produce two recoverable products: hydrogen and high-value carbon. Although a thorough review on the topic of methane pyrolysis can be found elsewhere [3], five primary pyrolysis methods are described below:

(i) Thermal decomposition: This method of carbon black production has long been used to produce a category of carbon black called “thermal black"[4], with

applications ranging from mechanical rubber goods like tires to synthetic polymers for electric equipment like cables and batteries. This method can consume H_2 produced via combustion for purpose of reactor heating and is not viewed as a means of H_2 production in this form. Resistive heating has also been explored some success, but challenges remain surrounding the scale up of the technology to be cost-competitive with SMR and his thus far not been commercialized.

(ii) Thermo-catalytic decomposition: Despite the moderate endothermicity of methane pyrolysis, a temperature above 1200 °C is required for pure thermal decomposition. Catalysts enable lower temperature methane conversion. This approach has been the subject of a great deal of research[5–8] . A large number of metal catalysts and carbonaceous scaffolds have been considered under different reactor configurations: fixed bed[9], fluidized bed[10], and vortex flow[11]. The most common catalysts are nickel, iron, copper, and cobalt, which all demonstrate catalytic activity for methane decomposition in the range 500-800°C[12]. These catalysts facilitate production of hydrogen and carbon nanostructures like nanotubes, nanofibers or graphene[13]. The main limitations of metal catalysts are their fast deactivation and the difficulty in separating them from the carbon products. To overcome these limitations, carbonaceous catalysts are also explored[14]. These are commonly in the form of amorphous high surface area carbons[15] and are active in the range of 800-900°C. These carbon catalysts are subject to deactivation as well, and may last longer than metal catalysts[16] but with lifetimes on the order of a few hours[17]. Strategies for solving this issue such as continuous regeneration of catalytically active carbons from catalytically inactive carbons are an active area of research[16,18].

(iii) Molten metal bath decomposition: This method has been the focus of intense research[19,20], and developments at the pilot level (e.g., C-Zero). It consists of bubbling methane through a column of molten metal. The methane contained in the bubbles is progressively decomposed during its ascent through the molten metal bath. Hydrogen exits the bath as an emanation gas while the solid carbon accumulates on the liquid surface. Depending on its nature, the metal may serve several roles: 1) to only facilitate heat transfer (Sn, Ga, Bi, Pb, etc.), 2) to facilitate heat transfer in the medium while preventing fouling, or 3) to facilitate heat transfer and catalysis (Ni, Fe, Co, Pd, Pt, etc.). Most catalytic metals have a melting point above 1000 °C (not far from the thermal methane decomposition threshold) while the inert ones have a melting point below 1000 °C. Challenges of this method include separating and recovering high-quality carbon, typically producing low-value morphologies contaminated by the metals used for the bath[21]. To our knowledge, the most advanced technologies remain at the pilot stage and no industrial process based on this technology has been achieved to date.

(iv) Concentration solar decomposition: Concentrated solar radiation can be used to heat reactor walls (indirect heating) to facilitate pyrolysis, or the solar radiation can be passed through a transparent boundary to facilitate pyrolysis of hydrocarbon gas commonly doped with a more radiative-absorbing component such as carbon particles [22]. A great deal of research in this area has led to important scientific advances in our understanding of nucleation mechanisms, particle growth, and radiative transfer in the presence of particles [23–25][25,26][11,27,28]. So far,

concentrated solar pyrolysis has not been commercialized. Notable challenges include rapid window clouding, poor thermal yield in the case of indirect heating, and the management and transportation of the solid carbon within and out of the reactor. Quality control of the carbon product and the cost of solar concentrators also remain important challenges for industrialization and deployment of this method.

(v) Non-thermal plasma decomposition: Research on non-thermal plasma pyrolysis is relatively early stage[29–35]. A non-thermal plasma is an ionized gas which remains at low temperature (tens to hundreds of degrees Celsius) because of its relatively low ionization rate but has significant chemical activity due to the presence of high-energy free electrons. Methane decomposition at lower temperature can be facilitated by electronic means. Different non-thermal plasma technologies including "gliding arc" and "cold arc" plasma technology have been proposed [31]. Notable progress in this area includes that by Atlantic Hydrogen, which was ultimately a unsuccessful commercialization venture [29,30]. Revitalized attempts at commercialization include efforts by Aurora Hydrogen (Canada).

2 Thermal plasma decomposition

Thermal plasmas allow electric to thermal energy conversion, with greater efficiency the larger the size of the installation[36]. In contrast to non-thermal plasmas, ionization rates are high enough to induce Joule heating. Thermal plasmas are a flexible and tunable heat source that can be free of CO2 emissions and are particularly suitable for endothermic processes. Commercialization of thermal plasma for hydrocarbon processing has been attempted for over 100 years, beginning with a patent by Rose in 1920[37]. From 1920 to 1990, many carbon black producers followed in the footsteps of the original thermal plasma process patent. Among them are Goodyear, Ashland Oil and Refining, Continental Carbon, and Phillips Petroleum. See Gonzalez et al. for a detailed history on the subject[38]. In the 1990s, the Norwegian engineering company Kvaerner (now Akker-Kvaerner) worked intensively on the development of a DC plasma technology for co-production of carbon black and hydrogen from natural gas. Initial efforts were conducted in collaboration with Sintef-NTNU Trondheim-Norway. In 1992, a plasma pilot of 3 MW was installed and successfully tested in Sweden in ScanArc installations in Hofors. In 1997, Kvaerner started the construction of the first industrial unit in Karbomont (Canada) with a capacity of 20,000 tons of carbon black and 6,000 tons of hydrogen per year. Unfortunately, the development of the technology was halted in 2003 due to technological problems and poor quality of the co-produced carbon black [39,40].

At approximately the same time, in 1995 Fulcheri et al. [41] presented a new concept on plasma methane pyrolysis for the CO2-free co-production of carbon black and pure hydrogen. Soon after, Muradov [42,43] and Steinberg [19] introduced the concept of fossil fuel decarbonization technology for mitigating global warming. This technology has been the focus of numerous patents and scientific articles[41,44–47]. Steam methane reforming has also been considered via thermal plasma[48–50]. A complete history of the evolution of this technology is documented by Fulcheri et al. [51]. This was followed by other research carried out by various

teams based in Canada, China, the United States and South Korea, which included work on laboratory devices based on different plasma technologies (i.e., induction, microwave, and arc). In 2012, after 30 years of intense and continuous lab and pilot scale R&D, the California start-up Monolith Materials, Inc. undertook the industrial development of this process for the co-production of carbon black and hydrogen in collaboration with the PERSEE team at MINES-ParisTech. A 1 MW pilot plant was successfully developed and tested from 2013 to 2018 in California. In 2018, MONOLITH initiated the construction of the first industrial production facility, Olive Creek 1 (OC1), located in Hallam, Nebraska, with a capacity to produce 14,000 tons and 4,600 tons per year of carbon black and hydrogen respectively.

The main advantage of the thermal plasma method is the ability to co-produce hydrogen and high value carbon black. Carbon black is a nanostructured material with a very high carbon content, generally higher than 95% by elemental composition. It is usually in the form of fine quasi-spherical particles, called "primary particles", which are generally connected together by covalent links to form aggregates, then agglomerates [4]. The average diameter of primary particles varies between a few tens and a few hundred nanometers depending on the production process. Some confusion may exist in the literature between the terms "carbon black " and "soot". The first refers to a material produced intentionally under controlled conditions, while the second refers to an undesired product of combustion that can be both hazardous to human health and have unintended environmental and ecological consequences. These two types of carbonaceous nanomaterials generally derive from very similar growth mechanisms.

Carbon black properties strongly depend on their synthesis conditions which include but are not limited to feedstock, heating medium, thermal histories, and reactor configurations. Their industrial applications depend on a large number of physicochemical parameters, which will not be described here. The nature of carbon black and it’s interaction with rubber has been the recent focus of Robertson and Hardman [52].

The formation of carbon black from methane pyrolysis is in essence the dehydrogenation process of different hydrocarbon compounds to a condensed phase, initiated through rupture of C-H bonds. Higher molecular weight alkene and alkyne particle precursors then form. Acetylene, particularly stable at high temperature, appears as a major precursor. In the next step, the first precursors react with each other to gradually form aromatic compounds, or polycyclic aromatic hydrocarbons (PAHs). Different PAH formation mechanisms have been identified, but the most widely known mechanism is denoted the H-Abstraction-Acetylene-Addition (HACA) mechanism [53,54]. This first stage of PAH collisions is known as nucleation, with nuclei comprised of 10-20 aromatic rings (although many nucleation mechanisms are hypothesized, discussion in this work is limited to that specific to carbon black formation). The next step leads to the formation of viscous tar nano-droplets by coalescing collision of nuclei. Maturation of particles occurs through an internal rearrangement of PAHs into turbostratic and graphitic layers, accompanied by a gradual loss of hydrogen within the particle and possibly continued mass addition via reaction of hydrocarbons at particle surfaces. Particles then progressively evolve from viscous to solid. Once this state is reached in most systems for carbon black production, the collision growth mechanism switches from a coalescing mode to a continuous aggregation process to form larger aggregates and agglomerates with a fractal

organization. Depending on the reactor type and configuration, all of the aforementioned processes may be happening simultaneously.

Industrial carbon black production started more than 100 years ago. Today, this industry is one of the top 50 chemical industries globally. The worldwide market is about 12 million tons per year for a revenue of about 15 billion USD. Most of this production is used in rubbers, mainly tires. **Figure 1** illustrates primary carbon black applications by industrial sector.

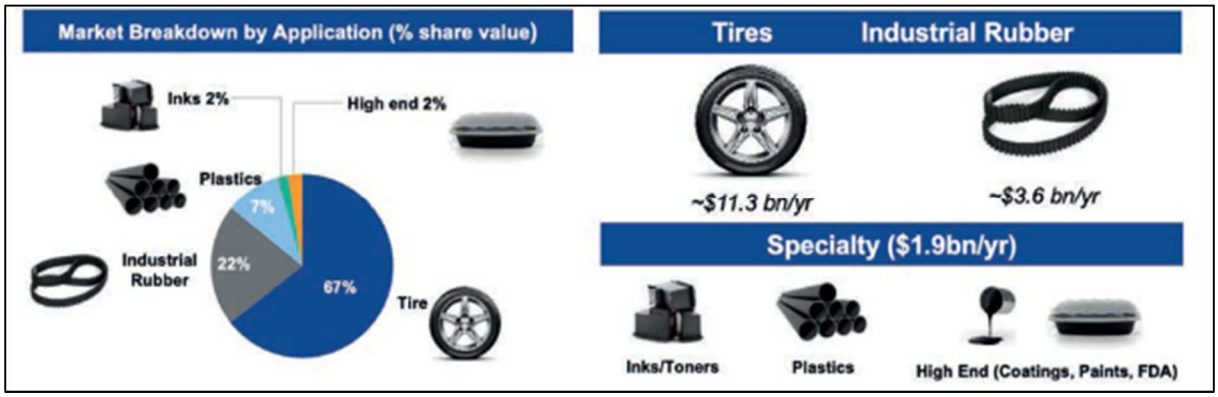

Figure 1: Carbon black applications represented by sector revenue (worldwide production: 16 million tons per year in 2017) [52]

Although thermal plasma decomposition has been well-documented in the literature, this work describes for the first time a process whereby high-value carbon black and hydrogen can be co-produced with high yields. There is no technology today other than thermal plasma decomposition of natural gas to carbon black and hydrogen that can provide yields of hydrogen and carbon black at greater than 95% each and also yield a high value carbon black with potential for replacing furnace black in automobile tires. This last item is key due to the fact that 75% of methane by mass is carbon and in order to make the most hydrogen possible, the largest carbon markets need to be addressed. By mass, 25 to 30% of a tire is carbon black and 65-70% of all carbon black that is produced by the heavily polluting furnace carbon black process goes into a tire.

3 Material and Methods

The experimental platform used in this work is shown in Figure 2 and is composed of the following parts: gas supply system, plasma source, pyrolysis reactor, filter system, water-cooling bench and output gas analysis bench. The gas supply system manages the routing of the input gases used in this work: hydrogen, nitrogen, carbon monoxide, argon and methane.

Nitrogen is first used as plasma gas before methane injection to heat-up the reactor until a thermal steady state is reached at a flow rate of around 30 Nm3/h. This operation generally takes around 2-3 hours. When the thermal steady state is reached, the plasma gas composition and flow rates are adjusted to the desired setting. Any plasma gas composition (pure or mixtures) can be achieved with the following gases: Argon, Hydrogen, Nitrogen due to three

separate mass flowmeters. There is no recirculation of gases from the exhaust of the lab scale unit back to the front end of the reactor making the lab scale unit a once through reactor system.
Simultaneously, methane is injected downstream of the plasma flow for initiating the pyrolysis process. The gas supply system includes a set of electronic valves, pressure regulators and mass flow controllers managed via a centralized digital control system. The plasma source is a three-phase plasma torch supplied by a multi-stage transformation power supply controlled in current mode and able to provide up to 250 kVA at 50 Hz. A thermodynamic equilibrium arc discharge is generated and alternates between the tips of three graphite electrodes producing a plasma typically at 2000+ degrees Celsius. Here, the graphite electrodes are progressively consumed during the process due to high temperature erosion. This erosion is relatively slow due to the extremely high thermal resistance of graphite. Consequently, the electrode holder was designed in such a way that the position of the electrodes in the discharge zone can be continuously controlled and adjusted to the erosion rate in real-time. The external boundary of the reactor is composed of a water-cooled double walled stainless steel vessel. The heat fluxes extracted by the cooling circuit are measured to fully define the energy balance of the system. The reactor has injectors especially designed for each gas which are distributed inside to impart mixing of the feedstock with the plasma gas. The quench gas utilizes pure Nitrogen to complete the system. Nitrogen is injected at a flow rate between 100-200 Nm3/h in the lower part of the reactor to cool down the gas to meet the thermal requirements of the filter assembly. The reactor is equipped with a large number of diagnostics and analytical devices such as temperature and pressure probes, optical pyrometry, electrical probes, high-speed cameras and optical emission spectroscopy (OES). A quartz window enables optical access for OES. The filter integrates a packaging device designed for automatic sampling of the produced carbon.
During the experiments, the following parameters were continuously recorded: r.m.s current and voltages for each of the three phases, feedstock and plasma gas flow-rates, input and output water temperatures in the cooling loops, water flow-rates for each cooling loop. The reactor internal wall temperatures were measured at different locations using optical pyrometers and Type C W-Rh thermocouples. In this work, mean reactor temperatures are presented and include those taken along several axial locations spanning the length of the reactor.

Carbon black samples were analyzed by transmission electron microscopy (TEM) and scanning electron microscopy (SEM). TEM observations were performed using an FEI Tecnai Osiris TEM. Ultrasonic dispersion of the carbon black was carried out in chloroform according to American Society for Testing and Materials (ASTM) D3849. The suspension was dispersed on the surface of a 200-mesh copper grid supporting a hollowed carbon membrane.

After the filtering and before the extraction of the produced gas, gas sampling is performed for continuous analysis during experimentation. This sample flow is delivered to a gas analysis bench which is composed of a set of devices enabling thermal conductivity detection (TCD), non-diffractive infra-red analysis (NDIR) and quantum cascade laser analysis (QCL). Quantitative measurements and concentration profiles in of the following chemical species are recorded: hydrogen, CH_4, C_2H_2, C_2H_4, C_2H_6 and carbon oxides (for the transient heat-up phase).

The target condition for each experiment is based on the variation of process parameters such as plasma power, mixture temperature, flow rates and dilution ratio, and by performing gas and solid carbon analyses. At each experimental condition, the solid carbon is separately recovered for analysis by Brunauer, Emmett, Teller (BET) method (giving an idea on the primary particles size), Dibutyl Phthalate (DBP) absorption (giving an idea on the aggregate structure), transmission of toluene extract (TOTE), X-ray diffraction (XRD), and TEM analysis (for overall morphology observation). Gas analysis is continuously performed during the experiment and elucidates the chemistry of feedstock conversion into hydrogen and carbon black - this analysis is crucial to determine *in-situ* process conversion rate.

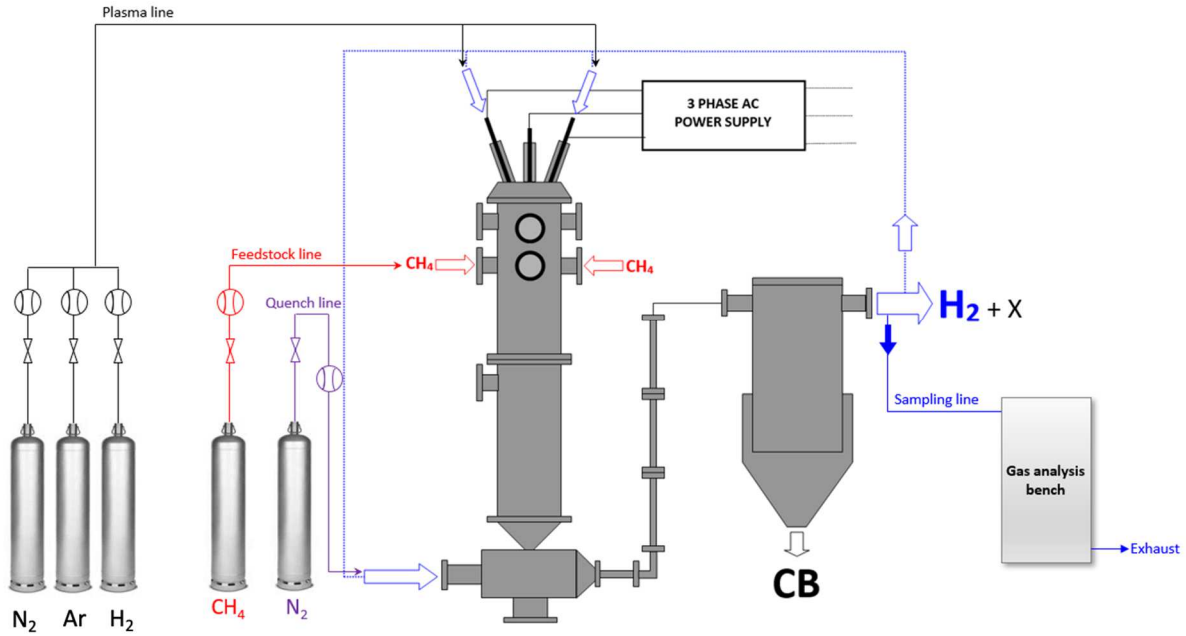

Figure 2: Experimental three-phase plasma methane pyrolysis bench utilized in this work.

4 Results

4.1 Experimental conditions

Table 1 below summarizes the experimental conditions of this work. A mixture of H2-N2 plasma gas was utilized for the conditions under the focus of this work. Two experimental conditions were studied, with similar process conditions. A volumetric flow dilution ratio (DR, defined below) of seven was used for both cases.

$$DR = \frac{total\ \ moles\ \ of\ \ diluent\ \ gas}{total\ \ moles\ \ of\ \ carbon\ \ injected} \qquad (2)$$

Mean reactor temperature varied by 100 C over the course of methane injection. Each experimental condition was run for roughly 40 minutes (allowing enough time for the generation of sufficient quantities of solid product for analysis), with reactor temperature generally increasing upon the start of methane injection. This phenomenon is due to the inception of particle-laden flow which enhances heat transfer via radiation and helps to transfer heat from the plasma to the product gas. In Case A, a quasi-thermal steady state is

achieved after 20 minutes. However, in Case B, more time was allowed for reactor heat up thus enabling a thermal steady state condition during methane injection. Reported energy intensities were computed from a heat balance through cooling water flows and thermal instrumentation.

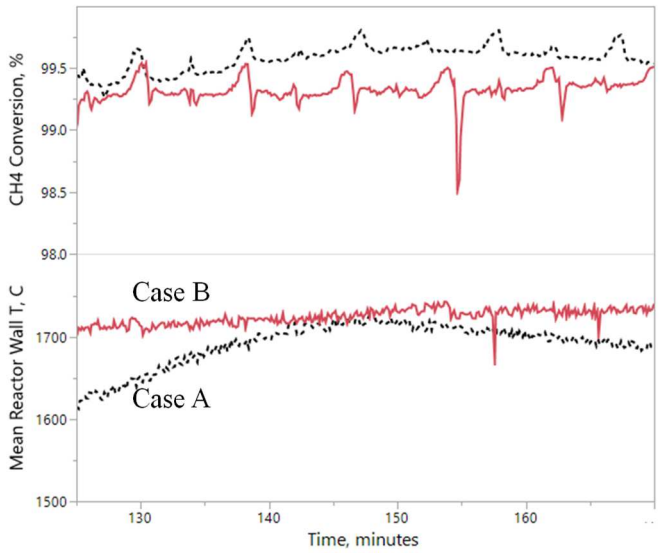

Figure 3. CH4 conversion time-histories and mean time-temperature histories for the conditions of this work. See Table 1 for description of cases (black dashed lines: Case A; red solid lines: Case B).

Table 1. Summary of experimental conditions investigated in this work. In both cases the following were fixed: plasma gas flow at 28 Nm3/hr with DR = 7.

Process Parameter	Case A	Case B
Mean Reactor Temperature, °C	1670	1710
H2-N2 in plasma gas	0-100	30-70
Mean Torch Power, kW	69	60
Total heat loss, kW	34	35
CH4 conversion, %	99.6	99.5
H2 yield, %	99	96
Total solid carbon yield, %	95	92
Energy Intensity kWh/kg H2	100	86
Energy Intensity kWh/kg Carbon	34	30

4.2 Methane conversion and product yields

Methane conversion and total solid yield are directly computed and estimated from measured flows and gas analysis instrumentation according to the following equation

$$X_{CH_4} = \frac{moles\ CH_4\ measured\ in\ process\ gas}{moles\ CH_4\ in\ feedstock} \quad (3)$$

Total solid yield is estimated from the following equation and integrated over the course of each individual condition:

$$X_{solid\ yield} = \frac{total\ mass\ carbon\ measured\ in\ system}{mass\ carbon\ in\ CH_4\ feedstock} \quad (4)$$

H2 yield is computed from the following equation:

$$X_{H_2} = \frac{moles\ H_2\ measured\ in\ process\ gas - moles\ H_2\ from\ plasma\ gas}{moles\ H_2\ in\ CH_4\ feedstock} \quad (5)$$

Methane conversion, solid carbon yield, and H2 yield are all presented in Table 1. Methane conversion in both cases is above 99%: 99.6% for Case A, and 99.5% for Case B. Both cases are economically favorable at commercial scale. As a result of the high methane conversion, the H2 yield for both conditions is also very high, at 99% and 96% for Cases A and B, respectively. The remaining hydrogen is contained in other gas phase hydrocarbons like C2H2, C2H4, and other species not measured by the gas analysis instrumentation.

Total elemental carbon balances were performed for each run and consider solid carbon mass produced and carbon mass flow in the exhaust, estimated by the gas analysis instrumentation. One limitation of this method of carbon accounting is that only several gas species are tracked. Hydrocarbons larger than ethane are not tracked and any such compounds formed and exiting the reactor do not take part in the carbon balance calculation. The remaining untracked carbon that does not convert to solid form is estimated based on gas analysis data and subsequent results of the carbon balance. This untracked carbon is computed to be 3% in both cases. Thus the possible error in the method of determining solid yield in this work is estimated to be ± 3%. The carbon balance for Case A is 100%, and 97% for Case B. The ability to close the carbon balances within 3% suggests that larger intermediate species like aromatics are not present in high quantities after the process gas exits the reactor. However, the inability to completely close the carbon balance for Case B supports the hypothesis of incomplete feedstock conversion and persistence of intermediate gas phase species which are not tracked by the gas analysis instrumentation.

4.3 Carbon product analysis

A comparison of solid carbon features analytically obtained is presented in Table 2, along with select examples from literature. While they do not provide a direct indication of how well the bulk solids will perform in industrial applications like rubber, they do provide a means of comparison with other ASTM standardized carbon blacks. It is assumed that reactor conditions can be further optimized and tuned to achieve a specific grade of carbon black. Both experimental conditions of this work produced bulk solid carbon at yields above 90%. X-ray diffraction was performed on bulk carbon samples from Case A, with results shown in Table 1. For comparison, the typical Lc values of carbon black produced by the furnace process are typically between 1-3. The surface area of the carbon produced here is in the

range of 90-110 m2/g, which is aligned well with those of furnace blacks using for reinforcing grade applications (80-100 m2/g). The concentration of toluene extractables is also on par with those from the furnace process.

Table 2. Comparison of select solid carbon analytical data with select furnace blacks (N660, N330) and acetylene black.

	Case A	Case B	N660	N330	Acetylene Black
XRD, Lc	3.0	N/A	1.2-1.5	1.2-1.5	25
d002,	0.35	N/A	0.35-0.36	0.35-0.36	
N2SA, m2/g	90-110	90-110	34	84	65
Mean primary particle diameter, nm	~30	~30	109	40	51
DBP, $cm^3/100$ mL	240	194	90	102	250
TOTE	99.6	100	>90	>90	

4.4 Particle morphology

TEM images were obtained for samples of Case A to investigate particle morphology. In general, the particles have aggregate morphologies common to carbon black, although the primary particles do not appear to be as spherical and turbostratic. This difference in appearance can be attributed to the higher reactor temperatures relative to the furnace process, as elaborated upon in previous work by Fulcheri et al.[44]

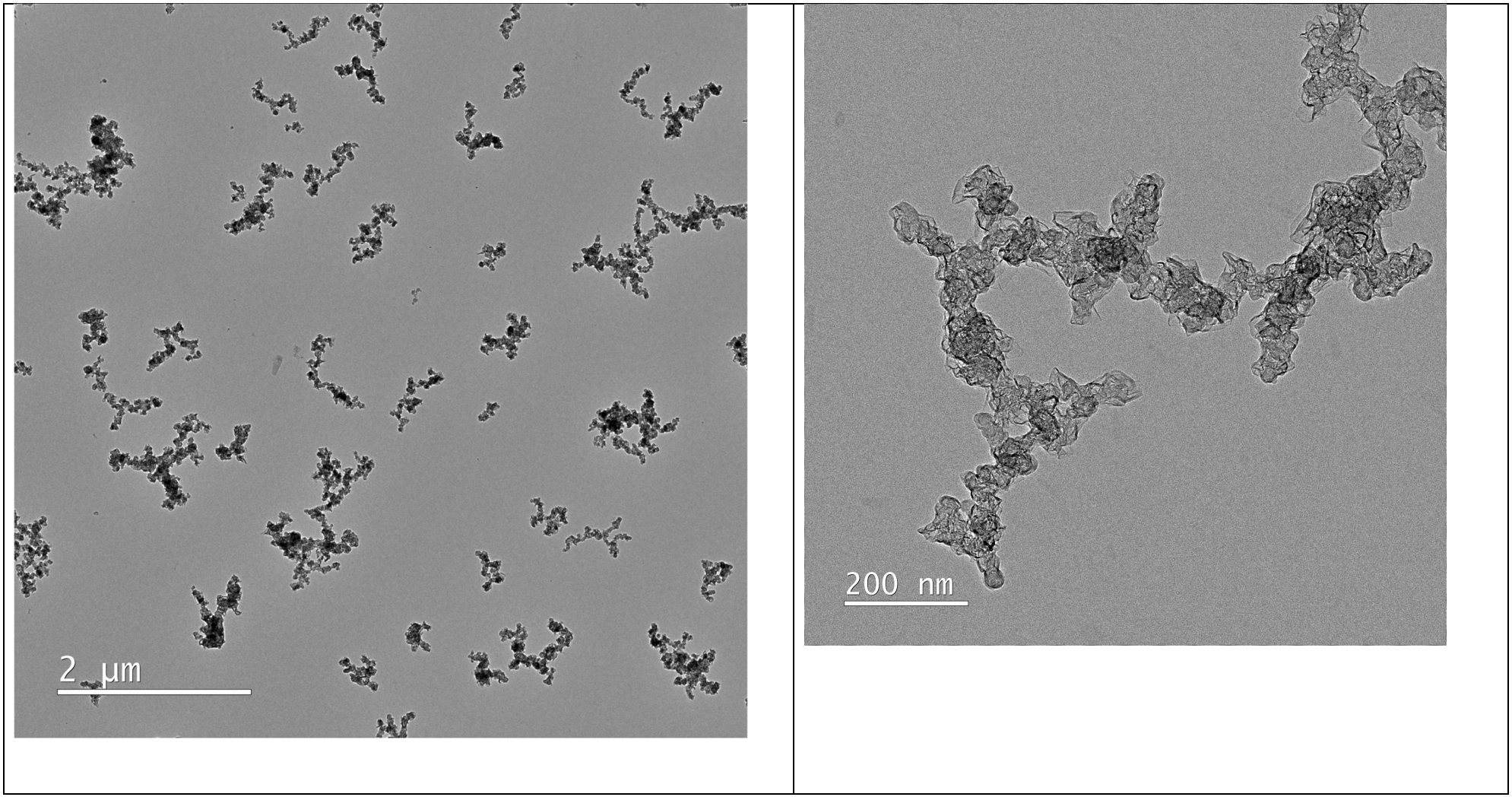

Figure 4. TEM images of carbon samples from Case A of this work.

4.5 Energy Intensity of the methane pyrolysis process

Considering the small scale of the 3-phase AC plasma system, energy intensity of the plasma pyrolysis system at this small scale is unsurprisingly very high since most of the energy is lost in water cooling circuits. According to Table 1, the energy intensity of hydrogen production was around 100 and 86 kWh per kg/H2 for case A and B, respectively.

As expected for high temperature processes, energy efficiency increases with scale.
Table 3 gives real-time operation data from Monolith Materials' Olive Creek 1 Plant: "OC1". OC1 will be followed by an additional 12 units of similar design at OC2 to produce an annual production capacity of 50 kilotons hydrogen and 180 kilotons carbon black. OC1 is the first and only commercial plasma methane pyrolysis plant in operation to date in the world. The energy intensity obtained at this scale is around 25 kWh per kg of Hydrogen which is extremely interesting considering this plant will not only produce hydrogen but also high value commercial grade Carbon Black. Despite the very early stage of this technology, the energy intensity is already only 42% of the energy intensity of water electrolysis which is around 60 kWh per kg of hydrogen. Noteworthy is that in addition to the hydrogen which is produced with an energy intensity of 25 kWh per kg Hydrogen, the thermal plasma process will also co-produce 3 kg of carbon black in an emissions-free manner that can replace the incumbent furnace black process.

Table 3. Olive Creek Plant Data for a yearly production of 50 kilotons of hydrogen and 180 kilotons of carbon-black (source: Monolith Materials)

Process Stage	Electrical Consumption
Plasma Reactor (Front-End)	Electricity: 1077 GWh/y
Carbon Black Back-End	Electricity: 34 GWh/y
Hydrogen Purification	Electricity: 96 GWh/y
Balance of Plant (BOP)	Electricity: 43.2 GWh/y
	TOTAL ELEC: 1250.2 GWh/y

5 Conclusions

Methane pyrolysis in various forms has been under development for decades, but commercial efforts have been thus far unsuccessful. This work documents - for the first time - characteristics of a commercial scale plasma methane pyrolysis process demonstrating high yield of both H_2 and high-value carbon: >95% and >90% respectively. Using data from an existing commercial scale system employing this process, an overall energy intensity of 25 kWh per kg of Hydrogen was calculated, representing 42% of the energy intensity for water electrolysis. Co-production of high-value carbon material in the form of carbon black has also been demonstrated for the methane thermal plasma pyrolysis process. Upon collection and analysis, the carbon produced via this method exhibits similar characteristics to commercial furnace black across several essential bulk particle properties, including similar morphology as assessed by TEM.

Hydrogen and carbon black are necessary inputs to many products that we consider to be essential today, fertilizer (via the Haber-Bosch process using H2 as a feedstock) and tires being two examples. Plasma methane pyrolysis is now a process demonstrated at commercial scale capable of producing both products with attractive characteristics such as high yield, high product quality, low energy intensity, and low carbon intensity [1].

References

[1] Liu K, Song C, Subramani V. Hydrogen and syngas production and purification technologies. John Wiley & Sons; 2010.

[2] Diab J, Fulcheri L, Hessel V, Rohani V, Frenklach M. Why turquoise hydrogen will Be a game changer for the energy transition. Int J Hydrog Energy 2022.

[3] Dagle R, Dagle V, Bearden M, Holladay J, Krause T, Ahmed S. An Overview of Natural Gas Conversion Technologies for Co-Production of Hydrogen and Value-Added Solid Carbon Products.(No. PNNL-26726; ANL-17/11). Pac Northwest Natl LabPNNL Richland WA U S 2017:65.

[4] Donnet J-B. Carbon black: science and technology. CRC Press; 1993.

[5] Bode A, Agar DW, Büker K, Göke V, Hensmann M, Janhsen U, et al. Research cooperation develops innovative technology for environmentally sustainable syngas production from carbon dioxide and hydrogen. 20th World Hydrog. Energy Conf., Gwangju Metroplolitan City (Korea): 2014.

[6] Meng X, Cui X, Rajan NP, Yu L, Deng D, Bao X. Direct methane conversion under mild condition by thermo-, electro-, or photocatalysis. Chem 2019;5:2296–325.

[7] Chen L, Qi Z, Zhang S, Su J, Somorjai GA. Catalytic hydrogen production from methane: A review on recent progress and prospect. Catalysts 2020;10:858.

[8] Qian JX, Chen TW, Enakonda LR, Liu DB, Basset J-M, Zhou L. Methane decomposition to pure hydrogen and carbon nano materials: State-of-the-art and future perspectives. Int J Hydrog Energy 2020;45:15721–43.

[9] Suelves I, Lázaro M, Moliner R, Pinilla J, Cubero H. Hydrogen production by methane decarbonization: carbonaceous catalysts. Int J Hydrog Energy 2007;32:3320–6.

[10] Muradov N, Chen Z, Smith F. Fossil hydrogen with reduced CO2 emission: modeling thermocatalytic decomposition of methane in a fluidized bed of carbon particles. Int J Hydrog Energy 2005;30:1149–58.

[11] Trommer D, Hirsch D, Steinfeld A. Kinetic investigation of the thermal decomposition of CH4 by direct irradiation of a vortex-flow laden with carbon particles. Int J Hydrog Energy 2004;29:627–33.

[12] Abbas HF, Daud WW. Hydrogen production by methane decomposition: a review. Int J Hydrog Energy 2010;35:1160–90.

[13] Amin AM, Croiset E, Constantinou C, Epling W. Methane cracking using Ni supported on porous and non-porous alumina catalysts. Int J Hydrog Energy 2012;37:9038–48.

[14] Muradov N, Smith F, Huang C, Ali T. Autothermal catalytic pyrolysis of methane as a new route to hydrogen production with reduced CO2 emissions. Catal Today 2006;116:281–8.

[15] Serrano D, Botas J, Guil-Lopez R. H2 production from methane pyrolysis over commercial carbon catalysts: kinetic and deactivation study. Int J Hydrog Energy 2009;34:4488–94.

[16] Dunker AM, Kumar S, Mulawa PA. Production of hydrogen by thermal decomposition of methane in a fluidized-bed reactor—Effects of catalyst, temperature, and residence time. Int J Hydrog Energy 2006;31:473–84.

[17] Muradov N, Smith F, Bokerman G. Methane activation by nonthermal plasma generated carbon aerosols. J Phys Chem C 2009;113:9737–47.

[18] Tabatabaieraissi A, Muradov N, Smith F. Process and apparatus for hydrogen and carbon production via carbon aerosol-catalyzed dissociation of hydrocarbons. US7588746B1, n.d.

[19] Steinberg M. Fossil fuel decarbonization technology for mitigating global warming. Int J Hydrog Energy 1999;24:771–7.
[20] Plevan M, Geißler T, Abánades A, Mehravaran K, Rathnam RK, Rubbia C, et al. Thermal cracking of methane in a liquid metal bubble column reactor: Experiments and kinetic analysis. Int J Hydrog Energy 2015;40:8020–33.
[21] Palmer C, Tarazkar M, Kristoffersen HH, Gelinas J, Gordon MJ, McFarland EW, et al. Methane pyrolysis with a molten Cu–Bi alloy catalyst. Acs Catal 2019;9:8337–45.
[22] Msheik M, Rodat S, Abanades S. Methane Cracking for Hydrogen Production: A Review of Catalytic and Molten Media Pyrolysis. Energies 2021;14:3107.
[23] Rodat S, Abanades S, Flamant G. High-temperature solar methane dissociation in a multitubular cavity-type reactor in the temperature range 1823– 2073 K. Energy Fuels 2009;23:2666–74.
[24] Rodat S, Abanades S, Flamant G. Co-production of hydrogen and carbon black from solar thermal methane splitting in a tubular reactor prototype. Sol Energy 2011;85:645–52.
[25] Hirsch D, Steinfeld A. Radiative transfer in a solar chemical reactor for the co-production of hydrogen and carbon by thermal decomposition of methane. Chem Eng Sci 2004;59:5771–8. https://doi.org/10.1016/j.ces.2004.06.022.
[26] Pratsinis SE, Vemury S. Particle formation in gases: a review. Powder Technol 1996;88:267–73.
[27] Abanades S, Flamant G. Production of hydrogen by thermal methane splitting in a nozzle-type laboratory-scale solar reactor. Int J Hydrog Energy 2005;30:843–53.
[28] Rodat S, Abanades S, Coulié J, Flamant G. Kinetic modelling of methane decomposition in a tubular solar reactor. Chem Eng J 2009;146:120–7.
[29] Fletcher DE. Production of hydrogen and carbon from natural gas or methane using barrier discharge non-thermal plasma. Patent No. US 20040148860A1, 2004.
[30] Boutot TJ, Liu Z, Buckle KR, Collins FX, Estey CA, Fraser DM, et al. Decomposition of natural gas or methane using cold arc discharge, Atlantic Hydrogen. WO2007/019664 A1, 2007.
[31] Czernichowski A., Czernichowski P., Ranaivosolarimanana A. Plasma pyrolysis of natural gas in gliding arc reactor. Proc 11th World Hydrog. Energy Conf, Stuttgart, Germany: 1996.
[32] Nozaki T, Kimura Y, Okazaki K. Carbon nanotubes and hydrogen co-production from methane using atmospheric pressure non-equilibrium plasma. Proc 16th ESCAMPIG 5th ICRP Jt. Conf, Grenoble, France: 2002.
[33] Oumghar A, Legrand J, Diamy A, Turillon N. Methane conversion by an air microwave plasma. Plasma Chem Plasma Process 1995;15:87–107.
[34] Wang Y-F, Tsai C-H, Chang W-Y, Kuo Y-M. Methane steam reforming for producing hydrogen in an atmospheric-pressure microwave plasma reactor. Int J Hydrog Energy 2010;35:135–40.
[35] Zamri AA, Ong MY, Nomanbhay S, Show PL. Microwave plasma technology for sustainable energy production and the electromagnetic interaction within the plasma system: a review. Environ Res 2021;197:111204.
[36] Boulos MI, Fauchais P, Pfender E. Thermal plasmas. vol. 1. Springer Science & Business Media; 1994.
[37] Rose JR. Process of and apparatus for producing carbon and gaseous fuel 1920.
[38] Gonzalez-Aguilar J, Moreno M, Fulcheri L. Carbon nanostructures production by gas-phase plasma processes at atmospheric pressure. J Phys Appl Phys 2007;40:2361.
[39] S. Lynum et al. Production of carbon black. WO-9320154, 1993.

[40] Gaudernack B, Lynum S. Hydrogen from natural gas without release of CO2 to the atmosphere. Int J Hydrog Energy 1998;23:1087–93.
[41] Fulcheri L, Schwob Y. From methane to hydrogen, carbon black and water. Int J Hydrog Energy 1995;20:197–202.
[42] Muradov NZ. CO2-free production of hydrogen by catalytic pyrolysis of hydrocarbon fuel. Energy Fuels 1998;12:41–8.
[43] Muradov N. Hydrogen via methane decomposition: an application for decarbonization of fossil fuels. Int J Hydrog Energy 2001;26:1165–75.
[44] Fulcheri L, Probst N, Flamant G, Fabry F, Grivei E, Bourrat X. Plasma processing: a step towards the production of new grades of carbon black. Carbon 2002;40:169–76.
[45] Gautier M, Rohani V, Fulcheri L, Trelles JP. Influence of temperature and pressure on carbon black size distribution during allothermal cracking of methane. Aerosol Sci Technol 2016;50:26–40.
[46] Gautier M, Rohani V, Fulcheri L. Direct decarbonization of methane by thermal plasma for the production of hydrogen and high value-added carbon black. Int J Hydrog Energy 2017;42:28140–56.
[47] da Costa Labanca AR. Carbon black and hydrogen production process analysis. Int J Hydrog Energy 2020;45:25698–707.
[48] Mašláni A, Hrabovský M, Křenek P, Hlina M, Raman S, Sikarwar VS, et al. Pyrolysis of methane via thermal steam plasma for the production of hydrogen and carbon black. Int J Hydrog Energy 2021;46:1605–14.
[49] Akande O, Lee B. Plasma steam methane reforming (PSMR) using a microwave torch for commercial-scale distributed hydrogen production. Int J Hydrog Energy 2022;47:2874–84.
[50] Choi DH, Chun SM, Ma SH, Hong YC. Production of hydrogen-rich syngas from methane reforming by steam microwave plasma. J Ind Eng Chem 2016;34:286–91.
[51] Fulcheri L, Fabry F, Takali S, Rohani V. Three-phase AC arc plasma systems: a review. Plasma Chem Plasma Process 2015;35:565–85.
[52] Robertson CG, Hardman NJ. Nature of Carbon Black Reinforcement of Rubber: Perspective on the Original Polymer Nanocomposite. Polymers 2021;13:538.
[53] Abid AD, Heinz N, Tolmachoff ED, Phares DJ, Campbell CS, Wang H. On evolution of particle size distribution functions of incipient soot in premixed ethylene–oxygen–argon flames. Combust Flame 2008;154:775–88.
[54] Dames E, Wang H. Isomerization kinetics of benzylic and methylphenyl type radicals in single-ring aromatics. Proc Combust Inst //;34:307–14. https://doi.org/10.1016/j.proci.2012.05.014.